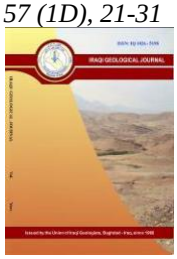
Iraqi Geological Journal

Journal homepage: https://www.igj-iraq.org



Mineralogy and Geochemistry Characteristics of Tanjero Formation in Selected Locations, Northeast of Iraq

Kareem Khwedim[1,] *and Zubaida A. Hameed[1]

[1] Department of Petroleum Geology and Minerals, College of Science, University of Diyala, Diyala, Iraq
* Correspondence: kkhwedim@gmail.com

Received:
11 August 2023

Accepted:
8 January 2024

Published:
30 April 2024

Abstract

Tanjero Formation (belongs to the upper cretaceous sequences(which are exposed in the northeast part of Iraq within the high folded zone. In this study, the mineralogy and geochemistry of the formation are examined by XRD and XRF techniques. The mineralogical study reveals that Calcite is the main mineral making the carbonate rocks of the formation with subordinate minerals of quartz and a low quantity of clay minerals (Chlorite, montmorillonite, and illite). Geochemical results revealed high levels of silica and calcium, aluminum, magnesium, and iron oxides. High concentrations of some trace elements (Cr, V) reflect their origin of basic and ultrabasic igneous rocks. The high content of Mn in the carbonate rocks of the formation reflects the depositional environment which is a deep marine environment. Most trace elements in the present study have positive correlations with SiO_2, Al_2O_3, and K_2O suggesting their association with clay minerals.

Keywords: Tanjero Formation; High folded zone; Clay minerals; Trace elements; Igneous rocks

1. Introduction

Tanjero Formation (Late Campanian-Maastrichtian) is predominantly made up of clastic sediments such as marl, siltstone, sandstone, shale, and conglomerate, according to Jassim and Goff (2006); Karim and Surdashy (2006) and Aqrawi et al. (2010), These clastic sediments formed as flysch deposits in a basin that was rapidly subsiding. The type section in Sirwan Valley, southeast of Sulaimaniyah, is divided into two sections: the upper section is made up of alternate bedding of silty marls, siltstone, conglomerates, and detrital limestone, with a thickness of up to 2010m; the lower section is made up of 484 m thick basinal marl, with some beds of limestone and siltstone (Sissakian et al., 2016). However, it becomes finer-grained and thinner-bedded as you move southwest. To the southwest, it becomes more finely grained and lightly bedded. The Balambo-Tanjero zone and a few locations in the low folded zone of the unstable shelf are the only places where the Tanjero Formation can be found.

The formation is exposed in certain regions and occasionally fills the troughs between the anticlines of the synclines (Sissakian et al., 2016). The lower part of the Tanjero Formation is conformable and gradational with the Shiranish Formation, whilst the higher boundary is unconformable with the Kolosh Formation. Many previous works deal with the petrographic characteristics of the Tanjero Formation to interpret the depositional environment. On the other hand, there is only one geochemical study on the formation in the study area by Al-Nakib and Dhannoun (2014), in which they pointed out the clear difference in the nature of the source rocks for the lower part of the formation compared to the upper

DOI: 10.46717/igj.57.1D.3ms-2024-4-13

part. The study showed that the lower part was deposited in deep marine basins, while the upper part was deposited in shallow basins.

The main objective of this study is to determine the mineralogical and geochemical characteristics, source rock, and correlation coefficient between geochemical elements of Tanjero Formation by conducting some geochemical and mineralogical analyses.

2. Materials and Methods

Twenty-four rock samples (12 from Dokan and 12 from Qamchuqa) were collected from two sections of the Tanjero Formation (Dokan and Qamchuqa) within latitudes (35°57’53.00, 35°53'29.39") N and longitude (44°54'7.00, "45° 0'45.51"E) (Fig. 1). Geochemical analysis was conducted to determine the percentages of major Element (SiO_2, Al_2O_3, Fe_2O_3, CaO, MgO, Na_2O, K_2O,TiO_2, LOI) and trace element (Cd, Co, Cr, Cu, Mn, Ni, Pb, V, and Zn) using X-Ray Flourescence (XRF) techniques and the analysis was carried out at the Iraqi- Germany Lab (Department of Geology, College of Science, University of Baghdad). While eight samples were selected to be analyzed for mineralogical analysis using XRD techniques to determine the mineralogical constituents, and it was carried out at the labs of the Ministry of Sciences and Technology.

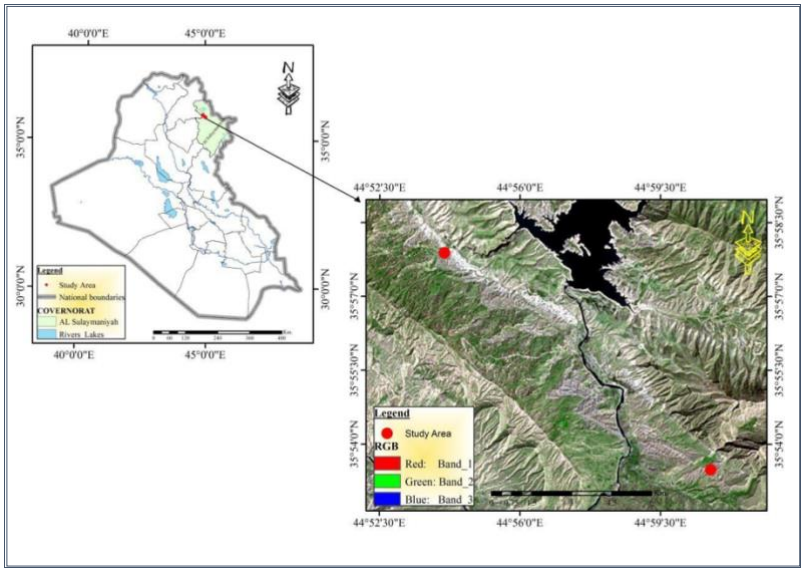


Fig. 1. Location of the study area (Google Earth maps).

3. Geological setting

The study area lies in the unstable shelf-high folded zone. Deformation from the Cretaceous and Tertiary eras significantly impacts this region. The cores of the anticlines contain limestones from the Mesozoic era, while their flanks contain limestones and clastic from the Tertiary era. In northeast Iraq and in the north of Iraq, the anticlines of this zone tend to extend in a trend of NW-SE and EW, respectively, according to Jassim and Goff (2006). Due to the closing of the Neo-Tethys, there was a significant marine incursion during the Late Campanian-Maastrichtian. NW-SE extensional basins were created as a result of the ophiolite obduction and the closure of the Neo-Tethys. In a foredeep basin that was subsiding at the time, ophiolite sheets that had been lifted above sea level were eroded and left behind as flysh deposits, which are represented by Tanjero Formation. As a result, the Balambo-Tanjero, high folded, and some low folded zones are largely covered by the Tanjero Formation. Shiranish carbonate and basinal marl are deposited laterally into the Hadiena, Aqra, and Bekhma Formations, which were deposited to the southwest in shallow environments.

4. Result and Discussion

4.1. Mineralogy

The results of XRD analysis showed that Dokan and Qamchuqa mudstones are composed of clay and non-clay minerals. Calcite was the most abundant mineral in the clay fraction of Tanjero Formation with an average of 45% (Table 1). It is identified in the range of 3.03 A° (Fig. 2), while the average of quartz is 41% (Table 1). It is identified in the range of d-spacing 4.25A° and3.33 A° (Fig. 2). Whereas Feldspar was identified at the peak of 3.19 °A in a small percentage in the study area (Table 1), compared with the calcite and quartz with an average of 3% (Fig. 2). The average of illite was 4% Table 1, and it can be identified by the basal reflection (001) d=10A°. The basic reflection of this mineral does not expand or collapse with respect to ethylene glycol when heated to 550°C (Faning et al., 1989) (Fig. 2). Weathering of silicates (mainly feldspar), metamorphism of other clay minerals, and degradation of muscovite give rise to the illite parentage, the predominant clay mineral in argillaceous rocks (Deer et al., 1975).

Illite minerals are alkali feldspar minerals, muscovite, and other alumino-silicates formed by direct weathering erosion or transformation, originating from acidic igneous and metamorphic rocks, and then migrated to sedimentary basins in the form of tiny clastic clays (Degnes, 1965 ; Grim, 1968 and Milott, 1970). This mineral is also formed by the weathering of ancient sedimentary rocks (Keller, 1962). Arid environments with low rainfall, high alkalinity (pH above 8.5), and rich potassium ions are ideal for Illite formation (Degnes, 1965). While the average of Chlorite was 45% Table 1 and can be observed in the basal reflections (001) and (003) at d=14-14.6 A° and d=4.7–4.9 A°, respectively, (Fig. 2). Fe-chlorite and the higher-order peaks may weaken while the (001) chlorites peak may increase significantly at 550°C of heating (Moore and Reynolds, 1997). Chlorite minerals are frequently found in igneous rocks as hydrothermal alteration by-products of ferromagnesian minerals and low grade greenschist facies metamorphic rocks (Deer et al., 1992). Montmorillonite mineral was identified in all samples of Tanjero Formation except sample D15. It is recognized in the basal reflection (001) at the range of d=14.2 - 15A° and the basal reflection 002 at 5.5 A° with an average of 4% (Table 1, Fig. 2). Montmorillonite is expanded when it is glycolated and the reflection present in d=17.18A°, and after heating to 550 C° the reflection is collapsed to 10 A°. This mineral is present in lower amounts compared to other clay minerals. Folk (1974) suggested that montmorillonite is usually developed in an Mg-rich environment and/or upon the weathering of Mg-rich ultrabasic rocks. It is most likely to form under conditions that are warm, dry, and poorly drained (Grim, 1968; Millot, 1970).

Table 1. Clay and non-clay minerals and their percentage (%) in Dokan and Qamchuqa sections in the Tanjero Formation.

Sample No.	Calcite	Quartz	Illite	Montmorillonite	Chlorite	Feldspar	Total
D15	58.1	29.4	5.9	-	4.6	1.9	99.9
D28	55.9	31.7	3.3	4.4	4.7	-	100
D29	13.3	68.6	4.0	4.5	4.6	5.0	100
Q2	33.2	50.5	3.5	5.2	4.1	3.5	100
Q7	56.6	31.2	3.3	2.2	3.3	3.4	100
Q9	59.0	28.2	1.8	4.5	4.5	2.0	100
Q10	25.8	57.4	4.7	3.2	5.1	3.8	100
Q16	55.4	29.1	2.4	5.6	3.5	4.0	100
Average	45	41	4	4	4	3	

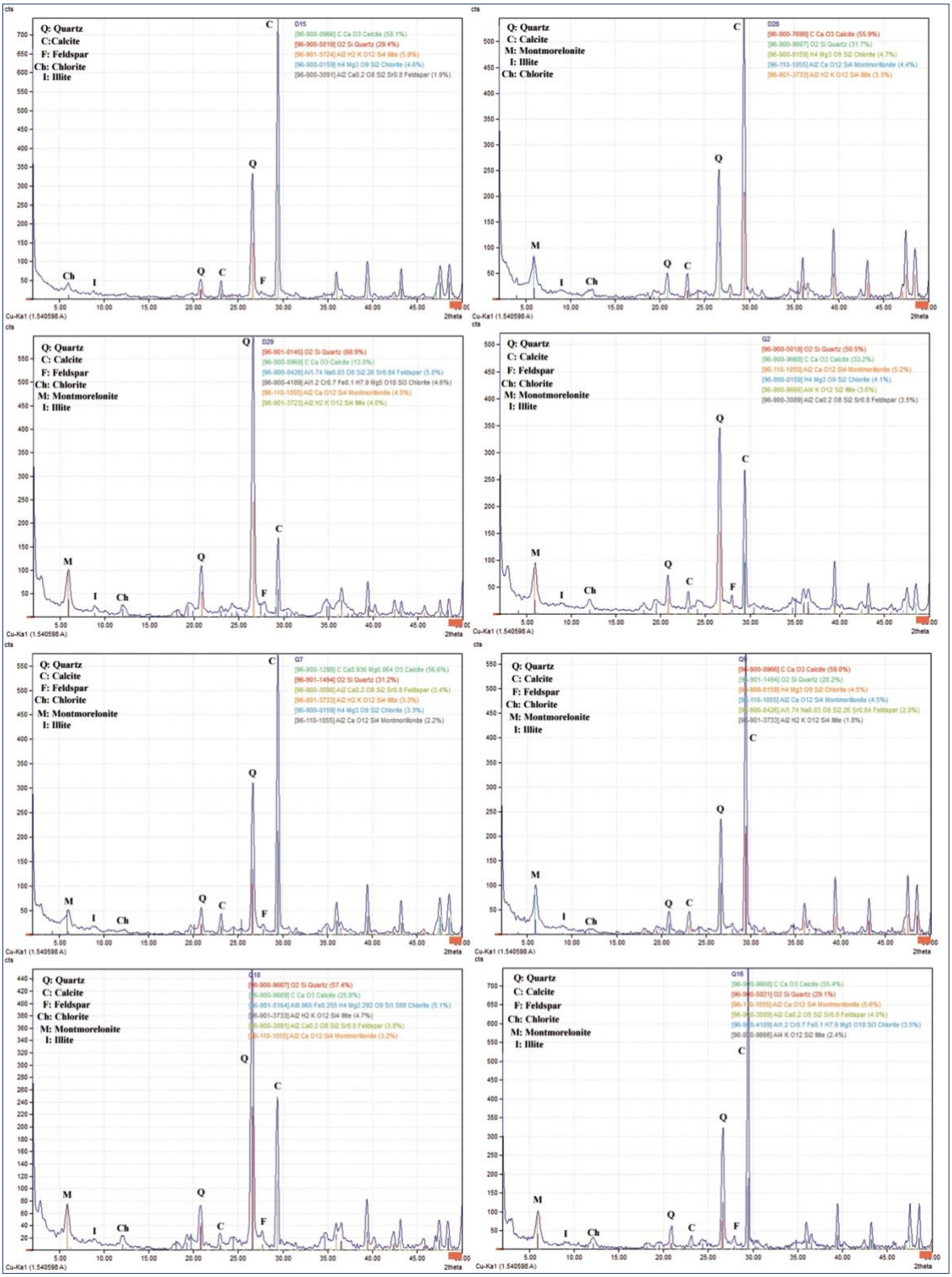


Fig. 2.X-ray difractogram of clay fraction of Tanjero Formation in Dokan and Qamchuqa sections.

4.2. Geochemistry

Twenty-four samples were selected for analysis from two sections (Dokan and Qamchuqa) of Tanjero formation for the determination of the major oxides (SiO_2, Al_2O_3, Fe_2O_3, CaO, MgO, Na_2O, K_2O,TiO_2, LOI) and trace element (Cd, Co, Cr, Cu, Mn, Ni, Pb, V, and Zn), The results and ranges of the chemical analyses for major and trace elements are listed in Tables (2 and 4).

4.2.1 Geochemistry of major oxides

The percentage of Silica in the Dokan section ranged from 21.23 to 41.65 , while it ranged from 18.26- 45.11 in the Qamchuqa section (Table 2). This low percentage may reflects the high content of carbonate rock fragments and ferromagnesian minerals and low content of quartz (Sarmad and Eman, 2018). Mud has more silica than other rocks, due to the presence of SiO_2 within the structure of clay minerals. In addition, carbonate cement will reduce the SiO_2 during replacement processes. Silica has strong positive relationships with Fe_2O_3 and positive with Al_2O_3, Na_2O, K_2O, and MgO but an inverse relationship with CaO because the depositional conditions of the calcium oxides differ from those of silica (Table 3). The silica is unstable in basic conditions (pH more than 7) so the silica dissolved in the mud (and vice versa) (Sadiq, 1985). While percentage of aluminum in the Dokan section ranged between 2.48 and 9.27, while it ranged between 3.74 and 9.63 in the Qamchuqa section, Table 2. Aluminum was a component of numerous minerals that arrived from rivers and wind sources. (Rubio et al., 2000) proposed aluminum as a resistant or stable element and one of the essential composites of clay minerals. The ratio of Iron oxide in the Dokan section ranged from 3.04 to 5.54 while its range in the Qamchuqa section was 3.03- 6.72 (Table 2). It is present in iron oxide-containing opaque minerals and makes up the majority of clay minerals including chlorite, montmorillonite, and kaolinite (Eslinger and Peaver, 1988; Sramek, 2000). It can exist as a matrix or as a coating around quartz crystals. It is transmitted as colloidal liquids and precipitated on the outer layers of clay minerals (Al-Samaani, 2011). Calcium is the most abundant oxide in the Tanjero Formation. Its range in Dokan was 24.1- 54.5, While in the Qamchuqa section 17.79- 54.3 (Table 2). The relatively high percentage of calcium oxides is due to the high content of carbonate rock in the Tanjero Formation, which is mainly composed of calcite, and the high percentage of MgO due to the presence of dolomitic limestone. Another source of calcium oxide is most probably coming from the weathering of pyroxene and amphibole minerals in the other locations. CaO is deposited in shallow environments in excess of carbonate, which increases in the expense of silica concentration (Omar and Al-Shamary, 2018). The percentage of Magnesium oxide in the Dokan section ranged from 3.01- to 6.22 while it is range in the Qamchuqa section was 2.54 and 7.09 (Table 2). The high percentage of MgO in the Tanjero Formation refer to the dolomitic limestone of this succession. While the low percentage of MgO comes from the existence of these oxides in the clay minerals like palygoreskite, chlorite, and montmorillonite (Omar and Al-Shamary, 2018). Sodium oxide in the Dokan section ranged from 0.22 to 2.97 whereas its range in the Qamchuqa section 0.23- 2.75 (Table 2).

The alkali (Na_2O and K_2O) contents mainly reflect the presence of detrital feldspar but also occur in clays (sarmad and Eman, 2018) (Table 3). Due to its effect on denudation operations and its simple movement as a result of its considerable solubility due to its low ionic potential, as shown in Tables (3 and 2), sodium oxide lacks a significant correlation coefficient when compared to other oxides (Glodshmidt, 1970; Mason, 1966). Potassium oxide in the Dokan section ranged from 0.18- 2.70 while its ranged in Qamchuqa 0.035- 2.39 (Table 2). The link between potassium and the other oxides is shown in (Table 4). There is a positive association between aluminum, silica, titanium, and iron oxides in the Dokan region, which suggests that it has entered the crystalline structure of the potassium feldspar, mica, and illite clay mineral (Tobia and Shangola, 2019; Avinash et al., 2016). K_2O reveals a strong positive relationship with Al_2O_3 because both elements are included in the crystalline structure of illite clay

minerals (Omar and Al-Shamary, 2018). The ratio of Titanium oxide in the Dokan section ranged from 0.023- 0.55 Dokan section whereas in Qamchuqa 0.032- 1.32 (Table 2). Al-Najjari (2019) reveals that Ilmenite ($FeTiO_3$), Rutile (TiO_2), and clay minerals chiefly montmorillonite contain significant amounts of Titanium oxide.

Table 2. Results of major oxides% of the studied succession.

Sample No.	SiO_2	Al_2O_3	Fe_2O_3	Na_2O	CaO	MgO	K_2O	TiO_2	L.O.I
D1	27.28	8.85	4.78	1.29	39.99	6.22	1.46	0.03	12.62
D4	41.65	6.03	5.54	2.61	24.19	3.30	1.59	0.23	14.16
D7	25.59	6.03	4.04	0.29	40.26	4.09	2.70	0.48	12.64
D9	38.79	9.27	4.26	2.31	30.69	4.32	1.08	0.49	12.45
D13	37.80	4.02	4.65	0.49	26.29	3.01	1.00	0.35	19.88
D15	39.64	5.69	4.26	0.40	24.13	4.29	0.59	0.37	20.14
D16	36.07	4.93	5.51	1.51	31.90	5.83	0.70	0.52	12.53
D19	28.20	4.70	4.96	2.97	45.81	5.09	0.60	0.39	10.61
D23	38.6	8.66	4.43	2.37	30.84	4.44	1.79	0.55	12.03
D26	22.47	5.44	3.04	0.91	50.52	4.10	1.00	0.02	13.5
D28	26.17	2.48	3.99	0.88	42.57	3.35	0.18	0.25	13.63
D31	21.23	8.66	3.14	0.22	54.55	3.51	1.73	0.50	18.26
Min	21.23	2.48	3.04	0.22	24.13	3.01	0.18	0.02	10.61
Max	41.65	9.27	5.54	2.97	54.55	6.22	2.70	0.55	20.14
Q1	18.26	5.24	3.03	1.17	54.30	2.54	0.33	0.79	15.8
Q2	38.46	4.03	5.41	2.36	24.58	3.72	0.64	1.32	17.73
Q7	28.43	9.63	3.48	1.44	38.35	4.54	0.33	0.51	12.35
Q10	45.11	6.69	6.52	0.54	17.79	7.09	1.18	0.52	13.34
Q12	37.09	4.54	5.64	0.23	30.88	4.91	1.79	0.33	14.41
Q13	36.25	3.74	4.19	0.85	30.81	5.36	1.00	0.03	16.01
Q14	27.86	9.47	4.78	1.36	37.87	4.96	0.38	0.61	12.22
Q15	23.09	9.25	4.55	2.12	38.74	6.19	1.02	0.05	14.91
Q16	36.24	5.86	5.92	1.19	29.67	5.62	0.04	0.05	14.52
Q17	38.10	7.77	4.18	1.25	29.54	4.76	0.03	0.05	12.78
Q20	37.57	4.50	6.72	2.75	24.62	4.18	2.39	0.70	15.78
Q22	30.73	7.77	4.86	2.58	36.05	5.30	1.48	0.76	9.78
Min	18.26	3.74	3.03	0.23	17.79	2.54	0.03	0.03	9.78
Max	45.11	9.63	6.72	2.75	54.30	7.09	2.39	1.32	17.73

Table 3. Correlation coefficient of major oxides in Dokan and Qamchuqa section (S.L. 0.5).

	SiO_2	Al_2O_3	Fe_2O_3	Na_2O	CaO	MgO	K_2O	TiO_2	L.O.I
SiO_2	1								
Al_2O_3	0.170	1							
Fe_2O_3	0.774	0.131	1						
Na_2O	0.388	0.388	0.498	1					
CaO	-0.316-	0.391	-0.194	0.214	1				
MgO	0.479	0.521	0.637	0.342	0.157	1			
K_2O	0.349	0.333	0.430	0.330	0.296	0.317	1		
TiO_2	0.343	0.222	0.413	0.458	0.223	0.128	0.350	1	
L.O.I	0.387	0.037	0.231	0.007	0.212	0.038	0.316	0.301	1

Concentration antinomy in titanium oxide is due to its ability to replace instead iron and aluminum, and according to the cation exchange capacity, which increases with the increase of clay minerals and the volume of clay (Al-Jubouri, 2005). LOI values were from 10.6 to 20.1 and 9.78 to 17.73 in Dokan and Qamchuqa sections respectively (Table 2). The LOI ratio comes from the loss of water content in gypsum and clay minerals as well as the CO_2 in carbonate minerals (limestone and dolomite) in the burning of samples (Omar and Al-Shamary, 2018).

4.2.2 Geochemistry of Trace Element

Vanadium (V) ranged from 24 to 531 ppm in Dokan whereas in the Qamchuqa 28 to 531 ppm (Table 4). V is adsorbed on clay minerals surface within the mineral structure or combined with iron oxides (Landergren, 1978). V found in ferromagnesium such as pyroxene and amphibole were altered to clay minerals (Omar, 2005). V shows a positive correlation with Zn, Cu, and Mn while it shows a negative to strong negative with Co, Ni, and Cr (Table 5). The range of chromium (Cr) was 40-2346 and 15- 2779 ppm in Dokan and Qamchuqa sections respectively (Table 4). Lithogenic Cr is inactive and harmless and is frequently exists in endured source materials like chromite and clay minerals as a replacement for octahedrally coordinated aluminum. Cr is a toxic element that occurs naturally and anthropogenically in soil (Becquer et al., 2003; Oze et al., 2004). Concern exists over Cr that is anthropogenically derived, particularly when it is detected in the hexavalent form. According to Gattullo et al. (2020), the metal differentiation between hexavalent and trivalent forms affects the soil toxicity of Cr. The increase of Cr because it is one of the remaining non-transitional elements during the weathering and transformation processes (Rose et al., 1979).

Manganese (Mn) ranges from 478.2 to 7481 ppm in Dokan and 196.4 to 2233 ppm in the Qamchuqa section (Table 4). Mn content in sedimentary rocks depends on the source rocks' geochemistry and the redox potential in the sedimentary environment (Goldberg and Humayun, 2016). Iron is usually associated with Mn due to similar geochemical behavior (Hylander et al., 2000) The abundance and distribution of Mn in carbonate sediments are considered a significant indicator utilized to recognize deep marine sediment from shallow, where Mn content is higher in the lithofacies of the deep marine environment than the facies of shallow environment (Shanmugen and Bendict, 1983). Mn shows a strong positive correlation with lead positive with zinc, cadmium, and copper, and negative with other elements (Table 5). Cobalt (Co) ranged from 3.9 to 206 and 3.9 to 202 ppm in Dokan and Qamchuqa respectively (Table 4). Pourret and Faucon (2018) revealed that Co is one of the components of numerous minerals like cobaltite, skutterudite, erythrite, spherocobaltite, and heterogeneity and it is common in igneous and sedimentary rocks. Co occurs naturally and resembles both iron and nickel in several ways. single stable isotope of cobalt exists in nature, where it coexists with other elements like oxygen, sulfur, and arsenic (Al-Saady, 2008). Strongly positive correlation with nickel and only a weak negative with zinc and lead (Table 4).

Nickel (Ni) was ranged between 18.1 and 2667 ppm in Dokan while 0.6 and 3132 ppm in Qamchuqa (Table 4). Ni is present with clay minerals and iron oxides in the sedimentary rocks due to the substitution and adsorption of magnesium and ferrous iron, or both (Bide et al., 2008). Ni shows a negative correlation with V and Mn and showed strong positive with Cr and Co (Table 4). A transition metal that is not present in great concentration in the crust of the earth. The most prevalent forms of it, oxides, were found in soil that contained serpentine. Copper exists in sediments as a replacement, adsorption on secondary iron and manganese oxides, clay minerals, or both, according to (Van Everbroeck et al., 2020). It ranges from 11 to 132.5 ppm in Dokan and (3.8-134.5) ppm in Qamchuqa (Table 4). Due to its high transferability, Cu is easily lost from clay during chemical weathering (Wedepohl, 1978). Zinc can also be found in sedimentary rocks as iron oxide and clay minerals (Berger et al., 2017). It is ranged between 41.3 and 154.7 and 26.4 and 145.2 ppm in Dokan

and Qamchuqa sections respectively (Table 4). Zinc shows a positive correlation with V, Mn, and Cu which indicates that these elements may come from the same sources, Table 4. Cadmium (Cd) ranged between 0 and 2 ppm in the Dokan section while it was 2 ppm in all samples of the Qamchuqa section (Table 4).

Table 4.The concentrations of trace elements (ppm) in Tanjero Formation (Dokan and Qamchuqa) sections.

Sample No.	V	Cr	Mn	Co	Ni	Cu	Zn	Cd	Pb
D1	372	296.7	1827	31.3	159	20.5	135.8	0	0.5
D4	388	337.4	1887	44.5	210.8	132.5	111.7	0.1	1.2
D7	176	942.4	1474	49.4	735.7	47.8	90.5	2	2
D9	382	187.6	2017	30	116.7	30.8	134.8	2	3.4
D13	160	343.3	4380	28	204.4	34.8	139.4	2	13.2
D15	150	731.4	7481	40.2	355.3	42.8	140.5	2	28.5
D16	268	303.5	1753	24.8	167.9	21.9	129.2	2	2.5
D19	531	243	2006	44.7	111.5	17	154.7	2	1.1
D23	94	40	691.4	19.8	97.6	19.9	118.2	2	8.8
D26	24	2346	874	206	2667	11	53.3	2	1.1
D28	209	56	478.2	3.9	18.1	23.6	41.3	2	3.1
D31	168	942.2	1498	52.9	750.3	45.9	82.4	2	1.6
Min	24	40	478.2	3.9	18.1	11	41.3	0	0.5
Max	531	2346	7481	206	2667	132.5	154.7	2	28.5
Aver	243.5	564.12	2197.2	47.96	466.192	37.38	110.98	1.6	5.58
Q1	295	341.7	1688	27.1	180.1	13.4	133.2	2	0.4
Q2	531	421.7	1773	42.6	102.1	134.5	113.5	2	4.7
Q7	153	1602	1896	98	1283	86.2	112.6	2	3
Q10	163	860.7	1313	117	611.5	52.7	139.7	2	14.7
Q12	143	1644	1437	133	1504	59.2	85	2	0.7
Q13	95	1.5	196.4	3.9	0.6	3.8	26.4	2	2.6
Q14	136	96.5	2115	26.9	132.5	45.9	100.7	2	9.7
Q15	38	2779	1311	184	3000	78.8	88.6	2	1.1
Q16	28	2758	821.7	202	3132	9.2	59.7	2	1.1
Q17	31	2711	1273	190	2886	78.5	78.7	2	1.1
Q20	168	806.1	2233	87	877	69.3	90.5	2	4.8
Q22	170	1222	2212	55	581.3	92	145.2	2	5.6
Min	28	1.5	196.4	3.9	0.6	3.8	26.4	2	0.4
Max	531	2779	2233	202	3132	134.5	145.2	2	14.7
Average	162.58	1270.3	1522.42	97.208	1190.84	60.29	97.816	2	4.125

Occurrence of Lead (Pb) is due to weathering, erosion, and deposition of crustal material, as well as Pb deposits released into the atmosphere of the Earth by eruptions, Pb is a naturally occurring element in the Earth's crust and can appear heterogeneously in soils (Callender, 2003; O'Connor et al., 2018). It is ranged from 0.5 to 28.5 ppm in Dokan and 0.4 to 14.7 ppm in Qamchuqa (Table 4). Pb showed a positive link with silica, iron, and aluminum oxides (Table 5), indicating that Pb is absorbed onto the clay particles' surface. The increase in Pb reflects the reducing conditions during the sedimentation period if they are suitable conditions for sedimentation. It shows a strong positive with Mn and a positive with zn and cd indicating that these elements may come from the same source, reflecting the high levels

of trace elements (Ni, and Cr) the origin of the prepared source rocks rich in these elements. These are the basal igneous rocks that contributed to the preparation of the clastics of the Tanjero Formation, as reflected in the rise of the ratios of these elements to the reducing conditions during the deposition period (Table 5).

Table 5. Correlation coefficient of trace element in Dokan and Qamchuqa section (S.L. 0.5).

	V	Mn	Cr	Co	Ni	Cu	Zn	Cd	Pb
V	1								
Mn	0.102	1							
Cr	-0.593	-0.150	1						
Co	-0.541	-0.214	0.953	1					
Ni	-0.622	-0.227	0.980	0.963	1				
Cu	0.229	0.111	0.161	0.113	0.061	1			
Zn	0.533	0.535	-0.343	-0.334	-0.435	0.166	1		
Cd	-0.374	0.001	0.202	0.166	0.192	-0.221	-0.172	1	
Pb	-0.137	0.789	-0.232	-0.222	-0.281	-0.006	0.377	0.193	1

5. Conclusions

The mineralogical study showed that calcite is considered the most common in the Tanjero Formation, followed by quartz. The percentages of clay minerals such as illite, chlorite, and montmorillonite were very low.

Silica and calcium, aluminum, magnesium, and iron oxides are considered basic components while alkali oxides (potassium and sodium) and titanium oxide are secondary components. Most major oxides of the Tanjero Formation showed diverse relationships that reflect various constituents and their sedimentary conditions and origins.

High values of some trace elements (Cr, and V) reflect their origin from the source rocks which are basic and ultrabasic igneous rocks. The high content of Mn in the carbonate rocks of the formation reflects the depositional environment which is a deep marine environment. Most trace elements in the present study have positive correlations with SiO_2, Al_2O_3, and K_2O suggesting their association with clay minerals.

References

Abdel-Kireem, M.R., 1986. Planktonic Foraminifera and stratigraphy of the Tanjero Formation (Maastrichtian)-northeastern Iraq. Micropaleontology Project Inc., 32 (3), 215- 231.

Aqrawi, A.A., Goff, J.C., Horbury, A.D., Sadooni, F.N., 2010. The petroleum geology of Iraq, Beacons field. Scientific Press Ltd, United Kingdom.

Al-Humaidan, Z.A. and Al-Jaberi, M.H., Al-Ali, R.A., 2019. A comparison of sedimentological, environmental, and fauna between two regions, NW of the Arabian Gulf. Mesopotamian Journal of Marine Science, 34 (1), 63- 84.

Al-Jobouri, M.A., 2005. Geochemistry of Coloured Argillites of Fat'ha Formation (Middle Miocene) and their Industrial Significance at Selected Areas in Northern Iraq. M.Sc.Thesis, College of Science, Mosul University.

Al-Najjari, N.A., 2019. Mineralogy, Geochemistry, and Provenance of Injana Formation in Selected Areas North-East of Iraq (Bazian, Quradagh, and Darbandikhan) and East of Iraq (Zurbatyah and Badra). Ph.D. thesis, College of Science, University of Basrah.

Al-Nakib, M.A., Dhannoun, H.Y., 2014. Impact of sharp changes in source rocks on the geochemistry of Tanjero Formation in Dokan district, northeast Iraq. Iraqi Bulletin of Geology and Mining, papers of the scientific Geological Conference part 1, 10 (2), 157- 172.

Al-Saady, Y.I., 2008. Environmental Geochemistry and Mineralogy of HorAlChekka southern of Al Msharrah river within Missan Governorate. M.Sc. thesis, University of Baghdad.

Al-samaani, J.J.A., 2011. Mineralogy and geochemistry of sandstone of Al-Mukdadiya Formation in selected areas, north-eastern Maysan. M.Sc. thesis, College of Science, University of Basrah.

Avinash, K., Kurian, P. J., Warrier, A. K., Shankar, R., Vineesh, T.C., Ravindra, R., 2016. Sedimentary sources and processes in the eastern Arabian Sea: insights from environmental magnetism, geochemistry, and clay mineralogy. Geoscience Frontiers, 7 (2), 253-264.

Becquer, T., Quantin, C., Sicot, M., Boudot, J.P, 2003. Chromium availability in ultramafic soils from New Caledonia. Sci. Total Environment, 301, 251- 261.

Berger, J.A., Schmidt, M.E., Gellert, R., Boyd, N.I., Desouza, E.D., Flemming, R.L., 2017. Zinc and germanium in the sedimentary rocks of Gale Crater on Mars indicate hydrothermal enrichment followed by diagenetic fractionation. Journal of Geophysical Research: Planets, 122(8), 1747- 1772.

Bide, T., Hetherington, L., Gunn, G., 2008. Nickel Definition, Mineralogy and Deposits. British Geological Survey.

Callender, E., 2003. Heavy metals in the environment-historical trends. Treatise on geochemistry, 9, 67- 105.

Deer, W.A., Howie, R.A., Zussman, J., 1975. An introduction to rock-forming minerals. Longman Group Ltd, London.

Degens, E.T., 1965. Geochemistry of sediments. A Brief Survey Prentice-Hall, New Jersey.

Eslinger, E., Pevear, D., 1988. Clay minerals for petroleum geologists and engineers. SEPM short course notes, Chapter 9, 22.

Faning, D.S., Keramidas, V.Z., El-Desoky, M.A., 1989. Micas, in Dixon, I. B, and Weed, S. B., Minerals in Soil Environment. Soil Science of America, Madson, WI, 551- 634.

Folk, R.L., 1974. Petrology of sedimentary rocks. Hemphill Publishing Co., Texas.

Gattullo, C.E., Allegretta, I., Porfido, C., Rascio, I., Spagnuolo, M., Terzano, R., 2020. Assessing chromium pollution and natural stabilization processes in agricultural soils by bulk and micro X-ray analyses. Environmental Science and Pollution Research, 27 (18), 22967- 22979.

Goldberg, K. and Humayun, M., 2016. Geochemical paleoredox indicators in organic-rich shales of the Irati Formation, Permian of theParaná Basin, southern Brazil. Brazilian journal of Geology, 46(3), 377- 393.

Goldshmidt, V.M., 1970. Geochemistry. Oxford University Press, London.

Grim, R.E., 1968. Clay mineralogy. 2nd ed. McGraw- Hill.

Hylander, L. D., Meili, M., Oliveira, L. J., de Castro E Silva, E., Guimarães, J. R. D. Araujo, D. M., 2000. Relationship of mercury with aluminum, iron and manganese oxy-hydroxides in sediments from the Alto Pantanal- Brazil. Science of the Total Environment, 260 (1), 97- 107.

Jassim, S.Z. and Goff, J.C., 2006. Geology of Iraq. Dolin, Prague and Moravian Museum, Brno. 341.

Karim, K.H. and Surdashy, A.M., 2006. Sequence stratigraphy of Upper Cretaceous Tanjero Formation in Sulaimaniya area, NW-Iraq. Kurdstan Academicians Journal 4 (1), 19- 43.

Keller, W.D., 1962. Diagenesis in Clay Mineral. Proceeding of the 11th Conference on Clay and Clay Minerals, 13, 136-157.

Landergren, S., 1978. Vanadium; In: Wedepohl K.W., Handbook of Geochemistry (ed.). Springer-Verlag, Berlin, 23, 1-10.

Masson, B. and Berry, L.G., 1966. Elements of mineralogy. John Wiley, New York.

Milot, G., 1970. Geology of clay. Springer-Verlag, New York.

Moore, D.N., Reynolds, R.C., 1997. X-ray diffraction and the Identification and Analysis of Clay Minerals. 2nd ed., Oxford University, 378.

O'Connor, D., Houm, D., Ye, J., Zhang, Y., Ok, Y. S., Song, Y., Tian, L., 2018. Lead-based paint remains a major public health concern: A critical review of global production, trade, use, exposure, health risk, and implications. Environmental International, 121, 85-101.

Omar, M., Al-Shamary, T.A., 2018. Sedimentology and basin development of the Miocene succession in the Zurbatiya area- Eastern Iraq. Iraqi Journal of Science, 59 (3B), 1409-1418.

Oze, C., Fendorf, S., Bird, D.K., Coleman, R.G. (2004). Chromium geochemistry of serpentine soils. International Geology Review, 46 (2),97- 126.

Rubio, B., Nombela, M. ,Vilags, A., 2000. Geochemistry of major and trace elements in sediments of the Ria de Vigo (NW- Spain). An Assessment of Metal Pollution. MarinePollution Bulletin 40 (11), 968- 980.

Sarmad, A.A., Eman, M.M., 2018. Geochemistry and provenance of sandstone unit in Tanjero Formation. Kirkuk Journal of Science, 13 (4), 113- 126.

Sadiq, A.J., 1985. Surface and subsurface mineralogical clays and iron ore in paleozoic rocks in the western. University of Baghdad.

Shanmugen, G., Bendict, G.L., 1983. Manganese distribution in the carbonate fraction of shallow and deep marine lithofacies, Middle Ordovician, Eastern Tennessee. Sedimentary Geology, 35 (3), 159-175.

Sramek, J., 2000. Compositional changes in Silurian shales conclusions based on calcite concretions. Research. University of Masaryk, (28), 89- 98.

Suttner, L.J., Dutta, P.K., 1986. Alluvial sandstone composition and paleoclimate, framework mineralogy. Journal of Sedimentary Petrology, 56 (3), 329- 345.

Sissakian, V.K., Abdul Ahad, A.D., Al-Ansari, N., Hassan, R., Knutsson, S., 2016. The regional geology of the Dokan area, NE Iraq. Journal of Earth Sciences and Geotechnical Engineering, 6 (3), 35- 63.

Tobia, F.H., Shangola, S.S., 2019. Geochemistry of sandstones from Beduh Formation in northern thrust zone, Kurdistan region, northern Iraq: provenance and tectonic setting. Iraqi Geological Journal, 52 (1), 15- 39.

Van Everbroeck, T., Ciocarlan, R.G., van Hoey, W., Mertens, M., Cool, P., 2020. Copper-containing mixed metal oxides (Al, Fe, Mn) for application in three-way catalysis. Catalysts, 10 (11), 1- 20.

Wedepohl, K.K., 1978. Handbook of Geochemistry. Berlin- Heidelberg- New Yor, Springer-Verlag, 2, Part 5.